

Systems biology

A computational model to predict the immune system activation by citrus-derived vaccine adjuvants

Francesco Pappalardo^{1,*†}, Epifanio Fichera^{2,†}, Nicoletta Papparone³, Alessandro Lombardo³, Marzio Pennisi⁴, Giulia Russo⁵, Marco Leotta¹, Francesco Pappalardo³, Alessandro Pedretti⁶, Francesco De Fiore⁷ and Santo Motta⁴

¹Department of Drug Sciences, University of Catania, ²Etna Biotech S.R.L, via Vincenzo Lancia, 57 - Zona Industriale Blocco Palma 1, ³Parco Scientifico E Tecnologico Della Sicilia, via Vincenzo Lancia, 57 - Zona Industriale Blocco Palma 1, ⁴Department of Mathematics and Computer Science, University of Catania, ⁵Department of Biomedical and Biotechnological Sciences, University of Catania, Catania, Italy, ⁶Department of Pharmaceutical Sciences, University of Milan, Milan, Italy and ⁷Softeco Sismat, Italy

*To whom correspondence should be addressed.

†The authors wish it to be known that, in their opinion, the first two authors should be regarded as joint First Authors.

Associate Editor: Jonathan Wren

Received on January 26, 2016; revised on March 18, 2016; accepted on April 20, 2016

Abstract

Motivation: Vaccines represent the most effective and cost-efficient weapons against a wide range of diseases. Nowadays new generation vaccines based on subunit antigens reduce adverse effects in high risk individuals. However, vaccine antigens are often poor immunogens when administered alone. Adjuvants represent a good strategy to overcome such hurdles, indeed they are able to: enhance the immune response; allow antigens sparing; accelerate the specific immune response; and increase vaccine efficacy in vulnerable groups such as newborns, elderly or immunocompromised people. However, due to safety concerns and adverse reactions, there are only a few adjuvants approved for use in humans. Moreover, in practice current adjuvants sometimes fail to confer adequate stimulation. Hence, there is an imperative need to develop novel adjuvants that overcome the limitations of the currently available licensed adjuvants.

Results: We developed a computational framework that provides a complete pipeline capable of predicting the best citrus-derived adjuvants for enhancing the immune system response using, as a target disease model, influenza A infection. *In silico* simulations suggested a good immune efficacy of specific citrus-derived adjuvant (Beta Sitosterol) that was then confirmed *in vivo*.

Availability: The model is available visiting the following URL: <http://vaima.dmi.unict.it/AdjSim>

Contact: francesco.pappalardo@unict.it; fp@francescopappalardo.net

1 Introduction

Vaccines are the most effective and cost-efficient means to prevent infectious diseases. Nowadays the approaches to develop novel and safer vaccines require the use of well-characterized antigens, such as purified proteins, peptides or carbohydrates. Unfortunately, often,

these so-called subunit antigens are poor immunogens when administered alone. Therefore, additional adjuvants are required to potentiate the immune response. Adjuvants can be used for various purposes: (i) to enhance, accelerate or prolong the immunogenicity

of highly purified or recombinant antigens; (ii) to reduce the antigen dose or the number of immunizations needed for protective immunity; (iii) to improve the efficacy of vaccines in high risk population such as newborns, elderly or immuno-compromised people; (iv) as antigen delivery systems for the uptake of antigens by the mucosa; and/or (v) to protect the antigens from degradation (depot effect). Adjuvants may also have significant effects on the nature of the immune responses, and can tilt the immune system in favor of T helper 1 (Th1) or T helper 2 (Th2) type response.

Adjuvants can be generally classified into two groups. The first group is composed of delivery vehicles that are used to manage the storage, releasing and presentation of vaccine antigens to the immune system. This group includes mineral salts, emulsions, liposomes and virosomes. The second group is composed of immunostimulants. Immunostimulants are compounds that aim to improve the immune responses to specific vaccine antigens by stimulating the releasing of cytokines through various mechanisms (i.e. MHC molecules, costimulatory signals or intracellular signaling pathways). In this group, it is possible to find Toll-like receptor (TLR) agonists, cytokines and saponins (Montomoli et al., 2011).

The first adjuvant activity was discovered empirically in 1926 with diphtheria toxoid absorbed to alum (Glenny et al., 1926). Since then, despite several decades of research, aluminium-based mineral salts (alum) remains the most used and approved adjuvant for human vaccines (Marrack et al., 2009). Alum has a good track record of safety and it has been considered the adjuvant of choice for vaccination against infections that can be prevented by antibody responses, and as such it has been widely and successfully used in many licensed vaccines. However, some limitations of alum are also well known. Alum fails to confer adequate increase of antibody response to small peptides as well as certain vaccines, such as typhoid fever and influenza vaccines. Notably, alum is known to be a poor adjuvant for induction of cytotoxic T cell immunity and Th1 responses, which are required to combat several life-threatening infections (Huckriede et al., 2005).

There is, then, an urgent need to develop novel adjuvants to support the development of vaccines against pathogens that have been so far refractory to the traditional vaccination strategies, to address effective vaccines against unmet medical need. In particular, the need of new adjuvants capable of boosting the immune responses of individuals with a lower or compromised immune system response, such as the elderly and immuno-compromised populations, represents a major challenge of our times.

Although a lot of effort has focused on the development of new adjuvants, which include mineral salts, detoxified toxins, lipopeptides, emulsions, cytokines, polysaccharides and nucleic acids, very few are presently approved for human use. There are in fact many issues that hinder the development of new adjuvants, including the development of local or systemic side effects. If the most common local reactions to adjuvants include pain, injection site necrosis, swelling, granulomas, lymphadenopathy, ulcers and abscesses, the most common systemic side-effects are represented by nausea, arthritis, fever, eosinophilia, uveitis, anaphylaxis, immunosuppression or autoimmune diseases (Allison and Byars, 1991). Even alum is not free from side effects such as fever and muscle soreness.

Moreover, difficulty of manufacture, poor stability and high production costs represent other unresolved issues of the adjuvant development pipeline. A deep scientific understanding of novel adjuvants is indeed compulsory to set up the required nonclinical safety testing programs, and even more testing programs are in general required for synthetic, nonhuman, derivatives of toxic compounds and protein-based adjuvants.

Accumulating evidence suggests that selected naturally derived components (such as, e.g. flavonoids and vitamins) collectively referred to as nutritive adjuvants have immunomodulating properties (Vajdy, 2011). Consequently, a good starting point for the development of new and potentially effective adjuvants may be to adopt naturally derived products, and their use may also lead to reduced toxicity and faster development.

There are many biotechnological methodologies for evaluating the efficacy of potential adjuvants, ranging from *in vitro* to *in vivo* techniques. Such techniques have often been coupled with the use of *in silico* techniques to speed up the identification of novel candidate adjuvants.

However, a complete pipeline encompassing initial selection (based on literature searches or *in vitro* studies), *in silico* evaluations at the molecular and cellular level, and *in vivo* trials, has yet to be developed.

The combination of *in silico*, *in vitro* and *in vivo* studies organized in a rationale manner at both molecular, cellular and systemic scales may represent major advance in the identification of potential novel adjuvants.

In this article, we present a computational framework that connects and integrates an *in silico* molecular evaluation, based on the virtual screening technique, with an *ad hoc* agent-based simulator to search and predict the best citrus-derived adjuvants able to enhance the immune system response. As a target disease model, we chose influenza A, using, as a candidate vaccine, the influenza A virosome. Finally, the predictions made by the simulation framework were validated *in vivo*.

1.1 The starting point: adjuvants derived from citrus

Plant extracts or purified component from plants have been evaluated for their activity as immunostimulant or immunomodulator, of which extracts from *Quillaja saponaria* Molina have proved the most successful when applied as a vaccine adjuvant. Indeed, the Quil A, a mixture partially purified of the crude extract of *Quillaja saponaria* Molina, is contained in several veterinary vaccines. A further purified saponin fraction named QS-21 is currently approved as a vaccine adjuvant for human use. Saponin fractions extracted from several other plants have been also tested as adjuvant with promising results, including Ginseng saponins, *Panax notoginseng* saponins, *Platycodon grandiflorum* saponins, Polygala saponins, soya saponins and many others (Hong-Xiang et al., 2009).

Although the chemical structure of phytosterols is very well known since 1922, their effects on human and animal health have been underestimated (Bouic, 2001). Among the phytosterols introduced by the diet, beta sitosterol is the most predominant sterol in the human herbal nutrition (Weihrauch and Gardner, 1978).

Hesperidin is an abundant and inexpensive by-product of citrus cultivation. It represents the major flavonoid in sweet orange and lemon (Garg et al., 2001). In the literature, there is some evidence to suggest that Hesperidin is a possible immunomodulatory compound in the vaccine field, with promising activity as an adjuvant (differential effect of hesperidin on Th1, Th2, Th17 and proinflammatory cytokines production from splenocyte of *Schistosoma mansoni*-infected mice (Gamal and Abdelaziz, 2013)).

2 Materials and methods

2.1 Virtual screening

Virtual screening is a powerful computational method that can be used to identify potential ligands for a specific biological target starting from a library of compounds. It can be classified into ligand based and structure based when the screening is performed by information contained in a pharmacophore model or by multiple docking

calculations. The former technique does not necessarily require knowledge of the biological target because the identification of the potential ligands is based on the molecular features needed for their recognition as activators or inhibitors. This set of molecular features is the pharmacophore model. Structure-based virtual screening is more expensive in terms of computational time, but can obtain more reliable results because the affinity of each candidate ligand with the biological target is evaluated by a scoring function. However, it requires the three-dimensional structure of the interaction partner; the most common source of experimentally resolved structures is Protein Data Bank, but although the number of structures it contains is growing, not all biological targets are available. Moreover, a virtual screening methodology is unable to predict and analyze the immune system dynamics as a whole.

A set of 148 molecules present in the essential oil of orange peel were collected (data not shown) by carrying out a systematic search in the primary literature. The three-dimensional structures were downloaded from PubChem (Bolton *et al.*, 2008) and for the molecules with unknown stereochemistry or geometric isomerism, all possible isomers were generated and considered as separate chemical entities. An extensive conformational analysis was carried out using the Boltzman Jump method implemented in AMMP software (<http://grid.cs.gsu.edu/~cscrrwh/ammp/ammp.html>) and the lowest energy conformation was further optimized by performing a semi-empirical calculation with the Mopac 2012 program (<http://OpenMOPAC.net>).

The crystal structure of the mouse TLR4/MD-2/LPS complex was downloaded from the Protein Data Bank (PDB ID 3VQ2) and was completed by adding hydrogens, fixing the atom charges using the Gasteiger–Marsili method (Ohto *et al.*, 2012) and the CHARMM 22 potentials for proteins (MacKerell *et al.*, 1998), using the features included in VEGA ZZ package (Pedretti *et al.*, 2002). After this step, the model was optimized through a conjugate gradients minimization (50,000 steps) to reduce the high-energy steric interactions, and to preserve the experimental data, atom constraints were applied to the protein backbone using NAMD 2.9 (Phillips *et al.*, 2005) integrated in the graphic environment of VEGA ZZ. Finally, LPS was removed from the complex to create the pocket required to identify LPS-mimetics by virtual screening calculations.

2.2 The influenza a conceptual model

The biological scenario and the dynamics of influenza A need to be described in a rational manner before they can be translated into a mathematical/computational description. This means that the description must capture the essential properties of the phenomenon, i.e. the system entities, how they are organized, and their dynamic behavior. The role of a conceptual model is then to drive biological knowledge into a solvable mathematical representation, offering a conceptual framework for thinking about the scientific domain and allowing the inclusion of additional properties in the same scheme with limited effort.

To satisfy the above properties, the first task in building a solid conceptual model is to identify all the relevant entities and their properties (cells, molecules, cytokines and interactions) that biologists and medical doctors recognize as crucial to the scenario. Next, one has to categorize all the interactions among entities that play a relevant role in the game. These must be described using biological knowledge inside a logical framework such that it is possible, as a further step, to map them from the biological world to a mathematical/computational one. The final step is to set all the biological

constants, relevant functions, and identify the optimal computational framework for hosting the simulated biological scenario.

The dynamics of cells is realized by state-changes: each cellular entity is labeled by a suitable state that describes its current biological condition (naïve, activated, duplicating and so on). The state can change when a cell interacts with another cell, with a molecule or with both of them.

We considered all the relevant lymphocytes that affect in some way the biological scenario. In influenza A, immune system response—both B lymphocytes and T lymphocytes—must be considered. Plasma B cells (P) were inserted as specific antibodies producers. Both cytotoxic T cells (TC) and helper T cells (TH) were inserted in the model. Monocytes are represented as well, as are macrophages (M). Dendritic cells play an important role in this infection. Two major types of dendritic cells have been discovered and have been named conventional (cDC) and plasmacytoid dendritic cells (pDC). pDCs are not able to present the antigen, so we represented only cDC in the model, along with their specific capability of processing and cross-presenting viral antigen peptides both in major histocompatibility complex class I (MHC-I) and major histocompatibility complex class II (MHC-II) molecules.

Toll-like receptors (TLRs) are a class of proteins that play a key role in the innate immune system. These receptors are usually expressed in sentinel cells such as macrophages and dendritic cells that recognize structurally conserved molecules derived from microbes. In particular, TLR-4 is able to recognize bacterial products, several viral proteins, polysaccharide and a variety of endogenous proteins such as low-density lipoprotein, beta-defensins and heat shock protein (Brubaker *et al.*, 2015).

We modeled the TLR-4 receptors in macrophages and dendritic cells to simulate their activation when triggered by citrus-derived adjuvants.

The Influenza A virus mainly infects the epithelium of the respiratory tract (Newby *et al.*, 2006) and its target is represented by epithelial cells (EPs). In spite of this, we did not model the dynamics of the EPs infected by Influenza A virus, but we tested the vaccination strategy using a virosome. Influenza A virosomes are virus-like particles, consisting of reconstituted influenza virus envelopes devoid of the nucleocapsid, including the genetic material of the source virus. Indeed, they contain functional viral envelope glycoproteins: influenza virus hemagglutinin (HA) and neuraminidase (NA) intercalated in the phospholipid bilayer membrane and they are unable to replicate and infect target cells, but act only as pure fusion-active vesicles (Huckriede *et al.*, 2005).

These functional characteristics of virosomes form the basis for their enhanced immunogenicity. It has been shown that a physical association between the virosome and the antigen of interest is necessary for the full adjuvant effect of virosomes (Bungener *et al.*, 2002). The repetitive arrangement of haemagglutinin molecules on the virosomal surface mediates a cooperative interaction between the antigen and Ig receptors on B lymphocytes, stimulating strong antibody responses. In addition, virosomes interact efficiently with antigen-presenting cells, such as dendritic cells, resulting in activation of T lymphocytes. The fusion of the virosomes with the endosomal membrane results in the major histocompatibility class I presentation pathway gaining access to part of the virosomal antigen, thus priming cytotoxic T lymphocyte activity.

In the light of these properties, virosomes represent an innovative, broadly applicable adjuvant and carrier system with prospective applications in areas beyond conventional vaccines, especially in stimulation of vaccine immunogenicity.

Natural killer cells (NK) have an important role in fighting virus-infected cells and tumor cells. However, some studies (Achdout et al., 2003, 2008) suggest that the influenza virus uses a novel mechanism for the inhibition of NK cell activity by means of MHC class I proteins redistributions on the cell surface and their accumulation in the lipid raft microdomains. This leads to better recognition by the NK inhibitory receptors and consequently amplifies resistance to NK cell aggression (Wang et al., 2000). It seems that this mechanism of evading NK cell attack does not affect T cell activity. At this stage, we did not take account of NK outcomes, as we did not have any infected EP cells.

Several molecular entities have an important role in simulating the influenza A infection scenario. The model distinguishes between simple small molecules, such as interleukins or signaling molecules in general, and more complex molecules, such as immunoglobulins and antigens, for which we need to represent the specificity. Regarding the interleukin class molecules, we represent interleukin 2 (IL-2) that is necessary for the development of T cell immunologic memory, one of the unique characteristics of the immune system, which depends upon the expansion of the number and function of antigen-selected T cell clones. As stated above, the model also takes into account interferons type I (both α and β). They drive two specific functions inside the simulation. The first is directed against the virus, inhibiting viral replication within the infected cell. The second function induces an antiviral state in surrounding cells (Stark et al., 1998). A mechanism for representing immunoglobulin class switching has also been incorporated. Immunoglobulins of both IgG1 and IgG2a are represented as well.

The model takes into consideration a 2D domain physical space, bounded by two opposite rigid walls and left and right periodic boundaries. Although this imposes a limitation in terms of the representation of space, all the processes and interactions of the simulated scenario take place in epithelium of the respiratory tract and in the surrounding lymph nodes. Hence, this is a good approximation and gives to the model implementation improvements in both speed and simplicity.

Using our previous experiences in the field of simulation of different pathologies and related immune responses (Castiglione et al., 2007; Palladini et al., 2010; Pennisi et al., 2015; Pappalardo et al., 2014), we chose to adopt an agent-based modeling (ABM) approach as a cellular computational framework. The advantages of this method are well known: both entities and biological functions and interactions can be described in terms that are very similar to the biological world. At the same time, this approach allows a mathematician or a computer scientist to describe the scenario using a logic and rational framework. Last but not the least, the ABM approach allows flexibility and further extension of the model to be achieved without significant additional effort.

Compared to the complexity of the real biological scenario of influenza A infections, the model is still naïve and it could be extended in many respects. However, the model is sufficiently complete and is able to describe the major aspects of the immune system response dynamics when stimulated by citrus-derived adjuvants.

2.3 The simulation framework

The simulation framework we developed is made of two main components. The first component is represented by the real simulator engine that we called SimFluAdj (SFA for short). The second component consists of an application that converts virtual screening results into simulation parameters that measure the affinity level of

the selected adjuvants against TLR-4. Figure 1 gives a general overview of the complete computational framework.

The computer implementation of SFA has three main classes of parameters: (i) values known from the standard immunology literature (Abbas et al., 2014); (ii) parameters strictly correlated with the specific biological scenario we want to simulate, i.e. parameters that measure the influenza A virosome dynamics, matching its behavior and its interactions with those of the host immune system (Baccam et al., 2006; Carrat et al., 2008; Doherty et al., 2006; Grayson and Holtzman, 2007; Lamb and Krug, 2001); (iii) parameters with unknown values which we set to plausible values after performing a series of tests. Table 1 details the values of the parameters retrieved from the literature, along with the specific parameters of the influenza A virosome. With the number of particles set to 100, it is able to generate an immune response that behaves as observed in literature (Huckriede et al., 2005).

SFA also has a set of free parameters that can be used to tune the model results with experimental data. The list of these parameters and their final values are quoted in Table 2. Tuning parameters were set using our previous experience in modeling and captured from discussions with biologists. The first parameter we set is *nbit_str* that determines the repertoire size. Its integer value determines the number of bits used to represent the molecules' and the cells' binding sites, such as cell receptors and antigen peptides and epitopes. *nbit_str* was set to 12, corresponding to a potential repertoire of 4096 possible cell receptors. This is obviously very limited in comparison to the real immunological repertoire, but it was sufficient to capture the global behavior of the influenza A infection process. The parameter *min_match* specifies the minimal number of matching bits that are required to have a non-zero probability for binding to occur; *affinity_level* is the probability of an interaction between two binding sites whose match is *min_match*; *max_lfact* regulates the probability that a duplicating cell will create a new cell; *IL2_eff* and *IFN1_eff* are factors expressing the efficiency of interleukin-2 in stimulating growth of the lymphocytes and the efficiency of IFN-1 in exploiting its function of antiviral effect respectively; *thymus_eff* represents the efficiency of the thymus in selecting

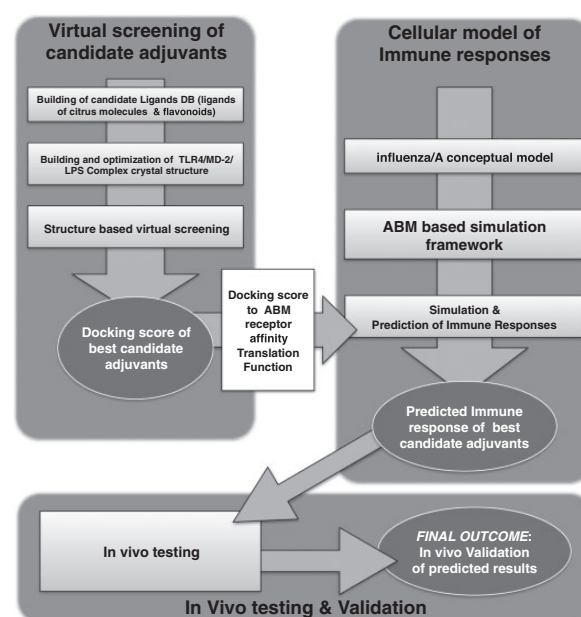


Fig. 1. Illustration of the general computational framework. Description...

Table 1. SFA parameters with known values retrieved from immune system specific literature

Entity	Initial quantity per μ l	Half life (days or h)
B	260	3.3 days
TH	876	3.3 days
TC	434	3.3 days
cDC	351	3.3 days
M	351	3.3 days
P	0	3.3 days
IC	0	4.0 days
IFN type I	0	1.6 days
IL-2	0	1.6 days
IgG1	0	23.0 days
IgG2a	0	23.0 days
Inf A virosome	100 particles	3.0 h

Table 2. SFA tuning parameters

Parameter	Value	Parameter	Value
Timestep	2 h	nbit_str	12
hyper_mut	10^{-4} in 8 h	min_match	9
plasma_rel	10 ng/ μ per 8 h	affinity_level	5×10^{-2}
prob_M_Ag	10^{-2} in 8 h	max_lfact	5
prob_M_IC	10^{-1} in 8 h	IL2_eff	100%
prob_cDC_Ag	2×10^{-2} in 8 h	IFN1_eff	100%
B_dup	16	thym_eff	99.9%
TH_dup	16		
TC_dup	16		

non self-reactive thymocytes. In general, the fraction of circulating auto-reactive TH cells should be below 0.1%.

With these settings, the model showed a good robustness, giving reasonable output. This means that if we slightly change parameters such as the initial leukocyte formula, the half life of entities, and so on, the model consistently varies its results, without biological discrepancy when compared with available experimental data retrieved from the above cited literature.

To take into account all time-related values, we set a time step of simulation to the value of 2 h.

Parameter *hyper_mut* is the per-bit mutation probability for antibodies. The hyper-mutation rate of antibodies is taken as the suggested value in Celada and Seiden (1996); *plasma_rel* controls the quantity of specific IgG antibodies directed against the influenza A virosome released by a plasma B cell at each time step; *prob_M_Ag* is the probability for a macrophage to phagocytose/internalize an antigen; *prob_M_IC* is the probability for a macrophage to phagocytose an immune complex; *prob_cDC_Ag* is the probability for a dendritic cell to phagocytose/internalize a virosome antigen. This was set to a higher level than the *prob_M_Ag* as DC are known to be more effective antigen presenting cells; *B_dup* is the number of time steps required by a B cells to create a copy of itself when duplicating; *TH_dup* is the number of time steps required by a TH cell to create a copy of itself when duplicating; *TC_dup* is the number of time steps required by a TC cell to create a copy of itself when duplicating.

SFA takes account of the main immune system functions and particular characteristics, such as the diversity of specific elements, major histocompatibility class restrictions, clonal selection by antigen affinity, thymus education of T cells, antigen processing and presentation (both the cytosolic and endocytic pathways are

implemented), cell–cell cooperation, homeostasis of cells created by the bone marrow, hypermutation of antibodies, cellular and humoral responses and immune memory. Receptors, ligands and immune system specificity are implemented in SFA by a *bit-string polyclonal lattice method*. This was well-described method and the interested reader can find additional information in specific literature (Farmer *et al.*, 1986; Motta *et al.*, 2005; Thorne *et al.*, 2007).

Immune system entities interact both with each other and with the cells and molecules of the body. From the point of view of biology, an interaction is a complex event that includes chemical, biological and dynamical actions. To capture the spirit of the entities' interactions, we adopt the same method that worked well in other cases we have simulated. We implemented both the recognition phase and the affinity eventually enhanced by adjuvants. When two entities that are capable of interacting lie in the same lattice site, they interact with a probabilistic law. All entities that may interact and are in the same site have a positive interaction.

The simulator takes care of the main interactions that happen during an immune response against influenza A infection. We included the following interactions.

2.3.1 B lymphocyte recognition of an influenza A virosome

If a B lymphocyte expresses on its surface a membrane immunoglobulin that is specific for the antigen, it internalizes the antigen complexed with the membrane immunoglobulin and turns the antigen into peptides that are presented by MHC class II molecules at the B lymphocyte surface. Hence, the lymphocyte B cell becomes an antigen presenting cell.

2.3.2 B lymphocyte and helper T lymphocyte interaction

If the T receptor (CD4) at the surface of a T helper lymphocyte binds specifically peptide/MHC-II at the surface of the antigen presenting B lymphocyte, the helper T lymphocyte proliferates and secretes interleukin 2. At the same time, B lymphocyte proliferates and differentiates into a plasma cell.

2.3.4 Macrophage and helper T lymphocyte interaction

If a T cell receptor (CD4) at the surface of T helper lymphocyte binds specifically peptide/MHC-II at the surface of antigen processing macrophage cell, helper T lymphocyte proliferates and secretes interleukin 2.

2.3.5 Macrophage and immune complex interaction

If a macrophage encounters an immune complex (specific IgG attached with influenza A virus), the macrophage phagocytoses the immune complex.

2.3.6 Macrophage with influenza A virosome

If a macrophage encounters influenza A virosome, the macrophage internalizes the antigen and processes it into peptides that are then presented by MHC-II at the macrophage surface. Hence, the macrophage becomes an antigen presenting cell.

2.3.7 Dendritic cell with influenza A virosome

If a cDC encounters influenza A virosome, the cDC internalizes the antigen and processes it into peptides that are then presented by MHC-II or by MHC-I (cross-presentation ability of cDCs) at the dendritic cell surface. Hence, the cDC becomes an antigen presenting cell.

2.3.8 Influenza A virosome with IgG interaction

If a soluble immunoglobulin specific for the virus encounters this antigen, it binds to it and forms an immune complex.

2.3.9 Cytotoxic T cell with antigen presenting cDC interaction

If a T cell receptor (CD8) at the surface of cytotoxic T lymphocyte binds specifically peptide/MHC- I at the surface of antigen-processing dendritic cell, the cytotoxic T lymphocyte become activated (primed).

Physical proximity is modeled through the concept of a lattice-site. All interactions among cells and molecules take place within a lattice-site in a single time step, so that there is no correlation between entities residing on different sites at a fixed time.

The simulation space is represented by an $L \times L$ hexagonal (or triangular) lattice (six neighbors), with periodic boundary conditions to the left and right side, while the top and bottom are represented by rigid walls. All entities are allowed to move with uniform probability between neighboring lattices in the grid with an equal diffusion coefficient. In the present release of the simulator, chemotaxis is not implemented.

The second component of the computational framework is represented by an application which integrates a translation function from the virtual screening docking scores into the corresponding bit-strings which are able to represent the same predicted affinity levels against TLR-4 receptors inside the simulator. This translation function has been obtained by initially defining the requested affinity levels for the SFA simulator, in terms of mismatching bits, for some of the predicted screening results (i.e. the best scoring = the maximum affinity). This data has been then used with a polynomial interpolation of the third order which fitted best with the input data in respect to other interpolation techniques we tested ($R^2 = 0.9062$). The resulting function is then used to obtain the number of mismatching bits that best represent any predicted virtual screening result, and thus to produce inside the SFA simulator string receptors with the requested number of mismatching bits.

2.4 Virosome preparation

A solution containing 1 mg of inactivated influenza A/H1N1 Singapore 6/86 was centrifuged for 90 min at $286,000 \times g$. The pellet was dissolved in 0.5 ml of PBS containing 0.1 M Octaethyleneglycol mono (n-dodecyl) ether (OEG) (Sigma Aldrich), and mixed with 32 mg of phosphatidylcholine (Lipoid Ag) dissolved in 1.5 ml of PBS - OEG 0.1M. The mixture was then centrifuged for 30 min at $100,000 \times g$ and the supernatant sterile filtered (0.22 m Millipore). Virosomes were then formed by detergent removal using SM2 Bio-Beads (Bio Rad). Final influenza hemagglutinin content was of 0.075 mg/ml, as determined by single radial diffusion.

2.5 Size determination

Size determination and distribution of the particle population was performed by a Zetasizer Nano instrument (Malvern Instruments). 20 μ l of virosome sample was added to filtered PBS buffer in a final cuvette volume of 1 ml. As shown (Fig. 2) the mean size of the influenza virosome is 117.6 nm with a polydispersity index of 0.1.

2.6 Mice and immunizations

Immunization experiments were performed in Balb/c mice (Harlan). Mice were housed in appropriate animal care facility and handled according to EU guidelines. Balb/c mice were randomly divided in the following groups (five mice per group) and labeled: group (A) PBS; group (B) virosome + hesperidin 1 μ g; group (C)

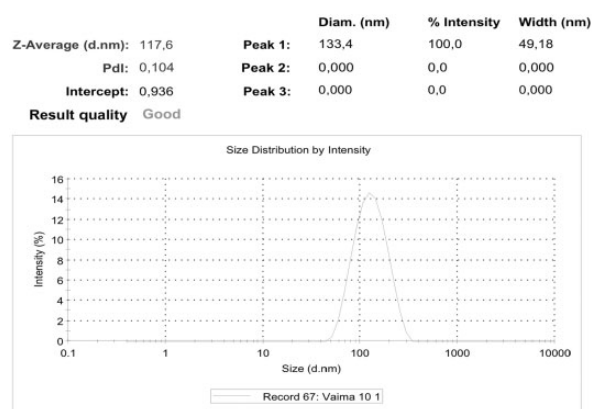


Fig. 2. Size determination. Zetasizer Nano instrument was used to determine the size determination

virosome + beta sitosterol 1 μ g; group (D) virosome + Linoleic ac. Ethyl est. 1 μ g; group (E) virosome without adjuvant. Animals were immunized two times at three weeks interval (days 0 and 21), and euthanized one week after the last immunization. Blood collection was performed at 35 days after the first immunization and sera samples were stored at -20°C till use. During the whole experiment, the animals were monitored and their weight recorded.

2.7 ELISA setting

Ninety six wells plates (Costar) were coated overnight at 4°C with 100 μ l per well of a 10 μ g/ml solution of whole inactivated influenza virus A/H1N1/Singapore Na₂CO₃ 0.05M pH 9.6. Wells were then blocked with 200 μ l per well of 10% milk powder in PBS solution for 1 h at 37°C , followed by one wash with PBS. Plates were then incubated with serial dilutions of the mouse serum in PBS containing 0.05% Tween 20 and 3% milk powder for 1 h at 37°C . After being washed three times with PBS containing 0.05% Tween® 20, plates were incubated with HRP-conjugated goat anti-mouse IgG, IgG1 or IgG2a antibody (Sigma-Aldrich) for 1 h at 37°C . After being washed three further times, 100 μ l TMB-substrate (Termo Fisher) was added, and the plates were incubated in the dark at room temperature for 15 min. The reaction was stopped by addition of 100 μ l 1M H₂SO₄ and optical densities (OD) were read at 450 nm using a Victor V (Perkin Elmer).

3 Results

The database of ligands for the virtual screenings was built from the molecules known in the literature to be found in orange fruit extracts, and their 3D structures were downloaded from PubChem, or built manually when not available. Moreover, to consider the possibility of finding ligands not yet identified or present in very low quantities in extracts, the database was merged with the molecules included in Arita's flavonoid library (Arita and Suwa, 2008) that were previously converted to 3D (Aldini et al., 2011). So, the final library consists of 6893 molecules in a Microsoft Access database. The structure-based virtual screening was carried out using the PLANTS software (Korb et al., 2009), defining a sphere of 12 Å radius centered on the LPS barycentre in its crystallographic pose and using PLP as the scoring function.

Betasitosterol, Linoleic Acid Ethyl Ester and Hesperidin were selected among the best ranked score candidate adjuvants because, as already detailed in Section 2.1, we found evidences of immune

Table 3. Virtual screening best ranked scores for the candidate adjuvants

Adjuvant	Score
Beta sitosterol	−102.682
Linoleic acid ethyl ester	−93.9251
Hesperidin	−95.096

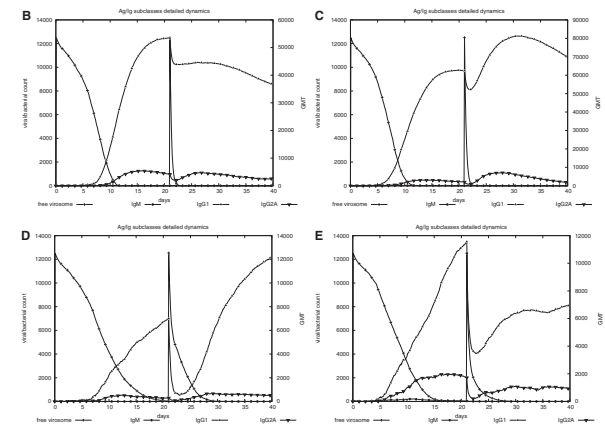


Fig. 3. Immunoglobulins class G subclasses detailed *in silico* dynamics. B – Hesperidin + virosome; C – Beta-Sitosterol + virosome; D – Linoleic Acid + virosome; E – Virosome only. Only beta sitosterol shows a good immune system humoral response, also at the time of the second administration, showing the typical burst-response (memory effect)

modulator effects. Table 3 shows the best-ranked adjuvants by score together with their scores.

The computational framework has been used to predict the administration of the proposed adjuvants over five virtual mice groups (Group (A) PBS + PC; Group (B) Virosome + Hesperidin 1 μ g; Group (C) Virosome + Beta-Sitosterol 1 μ g; Group (D) Virosome + Linoleic Acid Ethyl est. 1 μ g; Group (E) Virosome without Adjuvant). Fifty random simulations (random ‘in silico’ mice) have been executed for each group, and mean values have been taken into account. In Figure 2, we present the total IgG, IgG1 and IgG2a levels obtained at day 35.

According to the *in silico* predictions, the best adjuvant is represented by Beta-Sitosterol, which is capable of promoting a very strong humoral response when administered in conjunction with the virosome. A lower immune system response is also obtained by using hesperidin as the adjuvant, whereas the administration of linoleic acid did not bring any significant improvement in respect to the virosome administration only.

In Figure 3, we show the temporal evolution of IgG dynamics for virosome combined with Hesperidin (B), Beta-Sitosterol (C), Linoleic Acid (D) and virosome only (E). *In silico* simulations show that the administration of Linoleic Acid (D) seems to initially have a detrimental effect in respect to the administration of the virosome only (E). However, after the second immunization (day 21), a somewhat stronger immune response is capable of filling the gap between the two treatments, as highlighted by the behavior of IgG1 antibodies. Interestingly, both the administration of Hesperidin (B) and Beta-Sitosterol (C) are able to elicit a very strong first response but, as showed by IgG1 temporal dynamics, only the latter is able to improve the immune response after the second immunization, whereas the former partially loses its efficacy. We also report the dynamics of IgM titers; however, these levels were not measured in *in vivo*

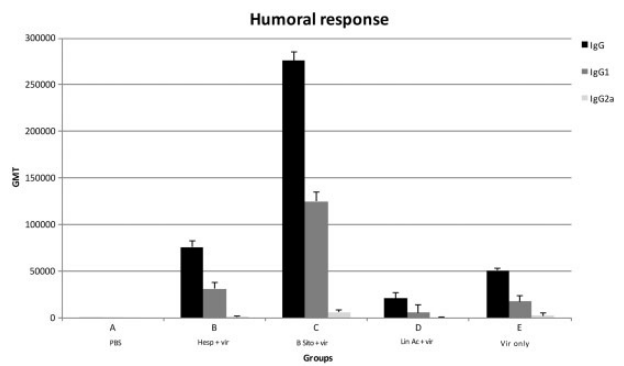


Fig. 4. *In vivo* results. Five groups of 5 balb/c mice were used. The first group (A) has no treatment (placebo); the second group (B) is treated with the influenza A virosome in conjunction with Hesperidin; the third group (C) is treated with the influenza A virosome in conjunction with beta sitosterol; the fourth group (D) is treated with the influenza A virosome in conjunction with linoleic acid; the fifth group (E) is treated with the influenza A virosome only. The levels of IgG, IgG1 and IgG2a are shown at day 35. Adjuvants dosage was of 1 μ g, administered at day 0 and 21. The experiments last 40 days. *In vivo* trials confirmed the predictions made by the *in silico* simulation framework

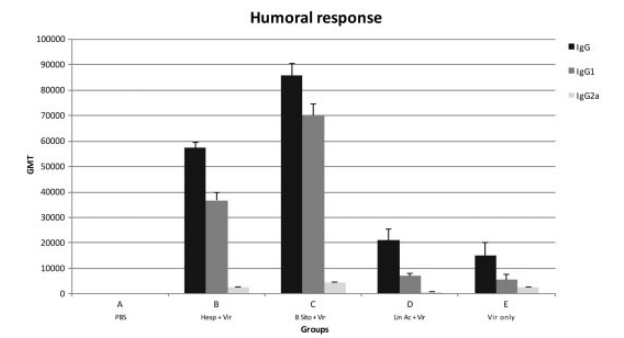


Fig. 5. *In silico* influenza-specific antibody titres. Five groups of 50 *in silico* mice were simulated. The first group (A) has no treatment (placebo); the second group (B) is treated with the influenza A virosome in conjunction with Hesperidin; the third group (C) is treated with the influenza A virosome in conjunction with beta sitosterol; the fourth group (D) is treated with the influenza A virosome in conjunction with linoleic acid; the fifth group (E) is treated with the influenza A virosome only. The levels of IgG, IgG1 and IgG2a are shown at day 35. Adjuvants plus virosome and virosome alone dosage were of 1 μ g, administered at day 0 and 21. The *in silico* experiments last 40 days

experiments. Hence, we used the same parameter values as in our previous works without tuning them. From a qualitative point of view, the low concentration of IgM may be in agreement with the general immunology literature. (Abbas *et al.*, 2014; Gonzalez-Quintela *et al.*, 2008).

In silico predictions have then been tested *in vivo* according to the procedure described in Section 2.6. In Figure 4, we show the IgG levels obtained *in vivo* at day 35. From a comparison of the *in vivo* and *in silico* experiments (Figs 4 and 5) it is possible to confirm that the simulator is clearly able to capture the complexity of the problem by predicting Beta-Sitosterol as the best adjuvant of the pool. The predicted Hesperidin effects seem to be slightly over estimated. However, the *in vivo* experiment confirms that the use of Hesperidin as adjuvant has a positive effect in comparison to the administration of the virosome only, even if with less efficacy.

Finally, as showed by the *in silico* predictions, the use of Linoleic Acid is useless for promoting the immunization. Indeed, the *in vivo* results show that it negatively influences the effects of the immune

response. This was also partially highlighted by the SFA simulator, but only at the time of the first immunization.

4 Conclusions

The need to develop a new generation of vaccine adjuvants is now an imperative. This is in particular important for those vaccines based on subunit antigens that provide superior safety over traditional vaccines; however, they suffer from limited immunogenicity when administered alone. There are few licensed adjuvants on the market approved for human use. The majority of them are Aluminium based. Even if alum has a good track record in terms of safety, it has some well-known limitations, such as inadequate increase of humoral response to small peptides and a poor stimulation of cytotoxic T cell immunity and Th1 responses. The development of new adjuvants is associated with two key problems: relevant side effect and high production costs. Naturally derived compounds have been demonstrated to provide a noteworthy immune system stimulation with limited side effects. There are several biotechnological methodologies, based on both *in silico* and *in vivo* techniques, to study and suggest possible good naturally derived adjuvants candidates. However, they are not able, on their own, to quantify and analyze the immune system response globally. Computational simulations may help in solving these issues, but these need to be integrated with the *in vitro* and *in silico* molecular analyses. In this work, we presented an integrated evaluation pipeline framework that uses virtual screening technique to pre-select promising citrus derived compounds that showed a good TLR-4 stimulation effects. Then we analyzed these results with an agent-based simulator to evaluate globally the immune system response using the pre-selected adjuvants in conjunction with an influenza A virosome. The simulation framework predicted that among the tested adjuvants, beta sitosterol is the one that elicits a good immune response. Finally, we tested *in vivo* the predicted results, finding a good agreement. This shows that the proposed simulation framework may accelerate and enhance the search and the development of adjuvants that may both improve the overall vaccinations strategies efficacy and reduce undesirable side effects.

Acknowledgement

The authors would like to thank Dr. Adrian Shepherd for his valuable comments that help to improve the manuscript.

Funding

This work has been funded by PO FESR 2007–2013 Sicilia - Linea intervento 4.1.1.1, project VAIMA 'Valutazione delle attività immunostimolanti di molecole bioattive estratte da agrumi' CUP: G63F12000050004.

Conflict of interest: none declared.

References

Abbas,A.K. *et al.* (2014) *Cellular and Molecular Immunology*. 8th edn Elsevier, Philadelphia.

Achdout,H. *et al.* (2003) Enhanced recognition of human NK receptors after influenza virus infection. *J. Immunol.*, **171**, 915–923.

Achdout,H. *et al.* (2008) Influenza virus infection augments NK cell inhibition through reorganization of major histocompatibility complex class I proteins. *J. Virol.*, **82**, 8030–8037.

Aldini,G. *et al.* (2011) An integrated high resolution mass spectrometric and informatics approach for the rapid identification of phenolics in plant extract. *J. Chromatogr. A.*, **1218**, 2856–2864.

Allison,A.C. and Byars,N.E. (1991) Immunological adjuvants: desirable properties and side-effects. *Mol. Immunol.*, **28**, 279–284.

Arita,M. and Suwa,K. (2008) Search extension transforms Wiki into a relational system: A case for flavonoid metabolite database. *BioData Min.*, **1**, 1–7.

Baccam,P. *et al.* (2006) Kinetics of Influenza A virus infection in humans. *J. Virol.*, **80**, 7590–7599.

Brubaker,S.W. *et al.* (2015) Innate immune pattern recognition: a cell biological perspective. *Ann. Rev. Immunol.*, **33**, 257–290.

Bolton,E. *et al.* (2008) PubChem: integrated platform of small molecules and biological activities. *Ann. Rep. Comput. Chem.*, **12**, 217–241.

Bouic,P.J. (2001) The role of phytosterols and phytosterolins in immune modulation: a review of the past 10 years. *Curr. Opin. Clin. Nutr. Metab. Care*, **4**, 471–475.

Bungener,L.B. *et al.* (2002) Virosome-mediated delivery of protein antigens to dendritic cells. *Vaccine*, **20**, 2287–2295.

Carrat,F. *et al.* (2008) Time lines of infection and disease in human Influenza: a review of volunteer challenge studies. *Am. J. Epidemiol.*, **167**, 775–785.

Castiglione,F. *et al.* (2007) Optimization of HAART with genetic algorithms and agent based models of HIV infection. *Bioinformatics*, **23**, 3350–3355.

Celada,F. and Seiden,P.E. (1996) Affinity maturation and hypermutation in a simulation of the humoral immune response. *Eur. J. Immunol.*, **26**, 1350.

Doherty,P.C. *et al.* (2006) Influenza and the challenge for immunology. *Nat. Immunol.*, **7**, 449–455.

Farmer,J.D. *et al.* (1986) The immune system, adaption, and machine learning. *Physica D*, **22**, 187–204.

Gamal,A. and Abdelaziz,S.A.A. (2013) Differential effect of hesperidin on Th1, Th2, Th17, and proinflammatory cytokines production from splenocyte of *Schistosoma mansoni*-infected mice. *Centr. Eur. J. Immunol.*, **38**, 29–36.

Garg,A. *et al.* (2001) Chemistry and pharmacology of the citrus bioflavonoid hesperidin. *Phytother. Res.*, **15**, 655–669.

Glenny,A.T. *et al.* (1926) Immunological notes: XVII–XXIV. *J. Pathol. Bacteriol.*, **29**, 31–40.

Gonzalez-Quintela,A. *et al.* (2008) Serum levels of immunoglobulins (IgG, IgA, IgM) in a general adult population and their relationship with alcohol consumption, smoking and common metabolic abnormalities. *Clin. Exp. Immunol.*, **15**, 42–50.

Grayson,M.H. and Holtzman,M.J. (2007) Emerging role of dendritic cells in respiratory viral infection. *J. Mol. Med.*, **85**, 1057–1068.

Hong-Xiang,S. *et al.* (2009) Advances in saponin-based adjuvants. *Advances in saponin-based adjuvants. Vaccine*, **27**, 1787–179.

Huckriede, A. *et al.* (2005) The virosome concept for influenza vaccines. *Vaccine*, **Suppl 1**, S26–S38.

Korb,O. *et al.* (2009) Empirical scoring functions for advanced protein-ligand docking with PLANTS. *J. Chem. Inf. Model.*, **49**, 84–96.

Lamb,R.A. and Krug,R.M. (2001) Orthomyxoviridae: the viruses and their replication. In: Knipe,D.M., Howley,P.M. (eds) *Fields Virology Fourth Edition*. Lippincott, Philadelphia, USA, pp. 1487–1531.

MacKerell,A.D.J. (1998) All-atom empirical potential for molecular modeling and dynamics studies of proteins. *J. Phys. Chem. B.*, **102**, 3586–3616.

Marrack,P. *et al.* (2009) Towards an understanding of the adjuvant action of aluminium. *Nat. Rev. Immunol.*, **9**, 287–293.

Montomoli,E. *et al.* (2011) Current adjuvants and new perspectives in vaccine formulation. *Expert Rev. Vacc.*, **10**, 1053–1061.

Motta,S. *et al.* (2005) Modelling vaccination schedules for a cancer immunoprevention vaccine. *Immun. Res.*, **1**, 5.

Newby,C.M. *et al.* (2006) Influenza A virus infection of primary differentiated airway epithelial cell cultures derived from Syrian golden hamsters. *Virology*, **354**, 80–90.

Ohto,U. *et al.* (2012) Structural basis of species-specific endotoxin sensing by innate immune receptor TLR4/MD-2. *Proc. Natl. Acad. Sci. USA*, **109**, 7421–7426.

Palladini,A. *et al.* (2010) In silico modeling and in vivo efficacy of cancer-preventive vaccinations. *Cancer Res.*, **70**, 7755–7763.

- Pappalardo, F. *et al.* (2014) Induction of T cell memory by a dendritic cell vaccine: a computational model. *Bioinformatics*, **30**, 1884–1891.
- Pedretti, A. *et al.* (2002) VEGA: a versatile program to convert, handle and visualize molecular structure on windows-based PCs. *J. Mol. Graph.*, **21**, 47–49.
- Pennisi, M. *et al.* (2015) Agent based modeling of the effects of potential treatments over the blood-brain barrier in multiple sclerosis. *J. Immunol. Methods*, **427**, 6–12.
- Phillips, J.C. *et al.* (2005) Scalable molecular dynamics with NAMD. *J. Comput. Chem.*, **26**, 1781–1802.
- Stark, G.R. *et al.* (1998) How cells respond to interferons. *Annu. Rev. Biochem.*, **67**, 227–264.
- Thorne, B.C. *et al.* (2007) Combining experiments with multi-cell agent-based modeling to study biological tissue patterning. *Brief. Bioinfo.*, **8**, 245–257.
- Vajdy, M. (2011) Immunomodulatory properties of vitamins, flavonoids and plant oils and their potential as vaccine adjuvants and delivery systems. *Expert Opin. Biol. Ther.*, **11**, 1501–1513.
- Wang, X. *et al.* (2000) Influenza A virus NS1 protein prevents activation of NF-KB and induction of alpha/beta interferon. *J. Virol.*, **74**, 11566–11573.
- Weihsrauch, J.L. and Gardner, J.M. (1978) Sterol content of foods of plant origin. *J. Am. Diet Assoc.*, **73**, 39–47.